Nanoscale Solution Structure and Transfer Capacity of Amphiphilic Poly(amidoamine) Dendrimers Having Water and Polar Guest Molecules Inside

Swapan Kumar Ghosh,[†,⊥] Seigou Kawaguchi,[*,‡] Yuji Jinbo,[§] Yoshinobu Izumi,[§] Keizo Yamaguchi,[‡] Tatsuo Taniguchi,[‡] Katsutoshi Nagai,[‡] and Kiyohito Koyama[†,‡]

Venture Business Laboratory, Yamagata University, Yonezawa 992-8510, Japan; Department of Polymer Science and Engineering, Faculty of Engineering, Yamagata University, Yonezawa 992-8510, Japan; and Graduate Program of Human Sensing and Functional Sensor Engineering, Graduate School of Science and Engineering, Yamagata University, Yonezawa 992-8510, Japan

Received March 11, 2003; Revised Manuscript Received September 18, 2003

ABSTRACT: Poly(amidoamine) (PAMAM) dendrimers of third and fourth generation (G3 and G4) are peripherally modified with hydrophobic stearyl acrylate via the Michael addition reaction. The hydrophobically modified dendrimers (**P3** and **P4**) are investigated to mimic the conventional inverse micelles in toluene medium by encapsulating organic polar dye Acid Red 1 (AR-1) and copper(II) salt from water phase to afford red and blue toluene phase, respectively. The efficacies of micelle-assisted transfer of AR-1 from aqueous solution into toluene phase are investigated, and the maximum numbers of dye loading per dendritic core are determined to be approximately 8 for **P3** and 24 for **P4**. The unimolecular natures as well as the structural characterizations of these dendritic inverse micelles in toluene before and after encapsulation of polar guest molecules such as water, AR-1, and copper(II) salt are studied by small-angle X-ray scattering (SAXS) experiments at 25 °C. The initial amphiphilic dendrimers of **P3** and **P4** have a globular structure in toluene and show scattering patterns similar to oblate ellipsoid of revolution with 17.7 and 25.9 Å in radius of gyration (R_g), respectively. Encapsulation of the polar guests such as water and AR-1 into the amphiphiles expands their chain conformation in toluene, and copper(II) salt increases the R_g value up to 34.5 Å for **P3** and 43.2 Å for **P4**. The scattering profiles of the expanded dendrimers are well described by those calculated from the sphere with a constant density.

Introduction

Dendrimers[1−4] with well-defined, highly branched architectures are potential candidates for well-varied technological applications including drug delivery, catalysis, gene therapy, light-harvesting antennae, chemical sensors, etc.[5−9] Most of the intended uses of dendritic macromolecules are designed on the basis of their two unique structural properties, namely large number of end functional groups and the nanoporous nature of the interiors. The possibilities of modification of the reactive peripheral groups with various functionalities have found enormous interest as a new model of potential amphiphilic materials having void space within their interiors. This can be used as a host to many nanosized chemical and biological molecules, catalytic sites of nanoscale reactions, and/or sequester ions.[10] The amphiphiles containing dendritic wedges also have found to act as unimolecular micelles,[11−13] exhibiting nanoenvironments similar to those encountered in conventional direct or inverse micelles from polymeric systems such as amphiphilic block or graft copolymers in a selective solvent, although the micelle formation by dendritic amphiphiles is thought to be independent of the concentration. Some normal[14−16] and reversed[17−21] dendritic unimolecular micelles have recently been reported in the literature. These compounds have also been recognized as effective tools for molecular encapsulation of guest, solubilizing the latter in a solvent of different polarity.[17,20,22−25] In reversed micelle category the most remarkable work was done by Meijer's group using poly(propyleneimine) dendrimers as the hydrophilic core.[17]

Another class of popularly available, commercial dendrimer, starburst poly(amidoamine)[1] (PAMAM) has a large enough interior to accommodate small molecules[26] and can also be easily modified peripherally, owing to the presence of a large number of reactive amino groups.[20,27,28] Furthermore, the presence of tertiary amine structure in the dendrimer building blocks makes this dendrimer a good sequester.[29]

In recent years studies have appeared in the literature about the hydrophobic surface modification of the dendrimers and their behavior at the air−water interface.[20,28,30] However, very little on their structural characterizations in solution state, especially in the presence of encapsulated guest molecules is documented. Amis and co-workers have reported cylindrical core−shell structural transformation of fifth generation poly(propyleneimine) dendrimer with stearyl groups filled with a gold salt hydrate $HAuCl_4 \cdot 4H_2O$ in toluene by small-angle neutron scattering (SANS) and small-angle X-ray scattering (SAXS) experiments.[21]

This paper reports synthesis of hydrophobically modified third (**P3**) and fourth (**P4**) generation PAMAM dendrimers with stearyl acrylates (SA) as hydrophobes via the Michael addition reaction (Scheme 1) and micelle-assisted transfer of polar guest molecules of Acid Red 1 (AR-1) and Cu(II) salt from aqueous phase to nonpolar organic phase, toluene. The structural characterizations of these amphiphilic dendrimers in a selective solvent, toluene, before and after encapsulation

† Venture Business Laboratory.
‡ Department of Polymer Science and Engineering.
§ Graduate School of Science and Engineering.
⊥ Present address: Pidilite Industries Limited, Mumbai, India.
* To whom correspondence should be addressed: e-mail skawagu@yz.yamagata-u.ac.jp, Tel, Fax 81- 238-26-3182.

10.1021/ma0343075 CCC: $25.00
Published on Web 10/28/2003

Scheme 1. Surface Modification of Starburst PAMAM Dendrimer (G3, 32 Surface NH_2 Groups) with Stearyl Acrylate via the Michael Addition Reaction

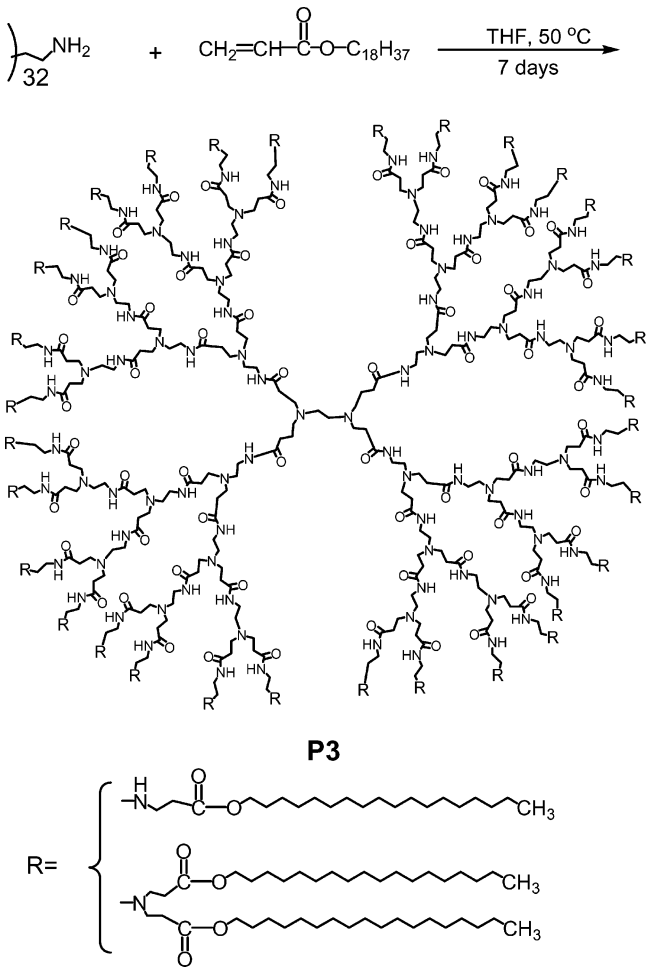

of water, AR-1, and Cu(II) salt have also been investigated by SAXS measurements and compared to the results of transfer experiments.

Experimental Section

Materials. PAMAM dendrimers, **G3**, 20.0 wt % solution in methanol, **G4**, 10.0 wt % solution in methanol (from Aldrich Chemical Co.), and SA (from TCI, Japan) were used as received. THF and toluene were distilled and dried by standard method just prior to use. Water purified by a Millipore Milli-Q purification system was used. Other chemicals like Acid Red 1 (Azophloxine, AR-1) (from TCI, Japan) and cupric nitrate trihydrate, $Cu(NO_3)_2 \cdot 3H_2O$ (from Kanto Chemical Co. Inc.) were used without further purification.

Synthesis. All the glassware was dried before use. 1.25 g of 20.0% **G3** PAMAM dendrimer solution in methanol (3.6×10^{-5} mol) or 2.5 g of 10.0% **G4** in methanol (1.8×10^{-5} mol), a sufficiently molar excess of SA (1.0 g, 3.08×10^{-3} mol), and 50 mL of dry THF were introduced in the reaction vessel, fitted with a condenser. The reaction was carried out under a nitrogen atmosphere and with magnetic stirring in a water bath at 50 °C. After 7 days reaction the solvent was evaporated, and the mixture was heated under reflux in 50 mL of diethyl ether for 30 min. It was then filtered to remove excess SA, and the same process was repeated thrice. The residue was treated thrice, each time with 50 mL of water under refluxing condition, to remove any water-soluble unreacted dendrimers present in it. The residue was then dried in a vacuum oven at 40 °C for 48 h, and the products were obtained as white solid materials. The products obtained (**P3** and **P4**) were insoluble in water, methanol, or diethyl ether but were highly soluble in chloroform, THF, and toluene.

Structural elucidation of **P3**: ^{1}H NMR[1,31] ($CDCl_3$): δ (ppm**)** 0.9 (t, CH_3), 1.2−1.75 (m, $-CH_2-)_{15}$, 1.6 (b, $-COO-CH_2-CH_2-$), 2.2−3.0 (m, all other $-CH_2$ of dendrimers if not specified otherwise), 3.2−3.4 (m, $-CONH-CH_2-$), 4.1 (t, $-COO-CH_2$). From the proton peak intensity ratio of $CONH-CH_2$ (of dendritic core) and $-CH_3$ (of hydrophobic chain) we quantified the presence of average 46 numbers of hydrocarbon chains per dendritic core (∼72% coverage, considering the defect-free starting dendrimer having 32 numbers of $-NH_2$ on the periphery as per the supplier specification). ^{13}C NMR ($CDCl_3$): δ (ppm**)**: 13.95, 22.54, 25.86, 28.52, 29.23, 29.49, 29.53, 29.59, 31.79, 32.61, 37.22, 49.12, 52.82, 64.66, 172.52, 172.79. FT-IR (KBr) peaks: (ν cm^{-1}) 3289, 3081, 2850, 1733 (C═O stretching vibration of $-CH_2-CH_2-COO-(CH_2)_{17}-CH_3$), 1645 (C═O stretching vibration of NH-*CO*), 1558, 1254, 1046, 721. Elemental analysis ($C_{1268}H_{2448}N_{122}O_{62}$): Calcd: C, 69.70; H, 11.21; N, 7.82. Found: C, 67.26; H, 10.96; N, 7.84. DSC: phase transition at 54.2 °C. Average molecular weight calculated from elemental analysis and ^{1}H NMR (46 hydrophobic chains): $(21.8 \pm 1.0) \times 10^3$. (GPC measurement with styragel column and THF as solvent was found to be difficult as the product stuck to the GPC column and not eluted properly.)

P4: ^{1}H NMR ($CDCl_3$): δ (ppm**)** 0.8 (t, CH_3), 1.2−1.5 (m, $-CH_2-)_{15}$, 1.8 (b, $-COO-CH_2-CH_2-$), 2.0−3.0 (m, all other $-CH_2$ of dendrimers if not specified otherwise), 3.2−3.5 (m, $-CONH-CH_2-$), 4.1 (t, $-COO-CH_2$), 7.0−8.2 (broad t, $-CONH-$). From the proton peak intensity ratio the presence of average 66 numbers of hydrocarbon chains per dendritic core were quantified (∼51% coverage, considering the defect-free starting **G4** dendrimer having 64 numbers of $-NH_2$ on the periphery as per the supplier specification). Elemental analysis ($C_{2008}H_{3888}N_{250}O_{256}$): Calcd: C, 67.68; H, 11.00; N, 9.82. Found: C, 64.94; H, 10.95; N, 9.45. DSC: phase transition at 54.9 °C. Average molecular weight calculated from elemental analysis and ^{1}H NMR (66 hydrophobic chains): $(35.6 \pm 2.0) \times 10^3$.

Measurements. ^{1}H NMR spectrum of the product was recorded on a JEOL 270 MHz NMR instrument using $CDCl_3$ as solvent. The Fourier transformation infrared (FT-IR) spectrum was recorded on a HORIBA FT-720 instrument. The elemental analysis data were obtained from a Perkin-Elmer 2400 II CHN analyzer. The phase transition temperature was measured in a Perkin-Elmer differential scanning calorimeter (DSC 7) at a heating rate of 10 °C/min. Karl Fischer titration experiments were carried out by laboratory made titration equipment under a nitrogen atmosphere. The micelle-assisted transfer of AR-1 and the complexing ability with copper ions were studied by using a UV-1600 UV−vis spectrophotometer (SHIMADZU). SAXS measurements were carried out at 25 °C, using BL-10C with a synchrotron orbital radiation as an X-ray source set up in the Photon Factory of the High Energy Accelerator Organization at Tsukuba, Ibaraki, Japan. The wavelength of the X-ray was 1.488 Å. The scattered intensity was recorded by a position-sensitive proportional counter (PSPC) with 512 channels over a scattering vector range from 0.02 to 0.30 Å^{-1}. The scattered vector was calibrated using a sixth peak of dry collagen. The details of the instrumentation and the procedure are described elsewhere.[32]

Results and Discussion

Micelle-Assisted Transport of Polar Dye AR-1 from Aqueous to Organic Phase. Guest−host properties of dendrimers or dendritic fragments are of great interest, and there are a lot of publications about this aspect, as summarized in a recent review.[33] A permeable dendritic core can accept guest molecules by constructing a dense shell around the impregnated core and forming a "dendritic box".[34−36] Another possibility is that the dendritic core of a preformed micelle-like host can be loaded with guest molecules in a homogeneous solution of both host and guest molecules.[17] Furthermore, some of the recent studies showed the dendritic

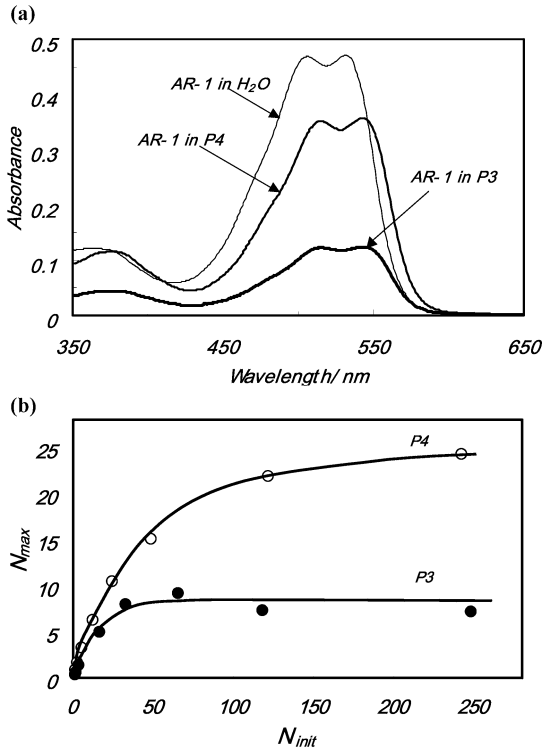

Figure 1. (a) UV−vis spectra of AR-1 aqueous solution (series 1) as well as in toluene phase after diffusion from aqueous phase with the help of **P3** and **P4**. (b) Occupancy of maximum number of dye molecules (N_{max}) per dendritic core with the varying initial molar ratio (N_{init}) of AR-1 and **P3** or **P4** in the aqueous/toluene phase.

micelle-assisted transfer of guest molecules between two immiscible phases.[20,25]

P3 and **P4** completely dissolve in toluene at room temperature, owing to the presence of hydrophobic stearyl chains on the periphery and might form reversed micelle-like structure, as will be discussed later. In this study we observed the transfer efficiency of **P3** and **P4** via their dendritic cores to a polar organic dye AR-1, from aqueous solution to an aromatic hydrocarbon solvent, toluene. When a clear toluene solution of **P3** or **P4** was layered on aqueous AR-1 solution, the color of the organic phase gradually changed to red, indicating the solubilization of the polar AR-1 with the dendrimers. UV−vis spectroscopic analysis was conducted to elucidate the amount of ionic dye AR-1 in the organic phase. A small red shift from 533 nm, the λ_{max} of aqueous AR-1 solution, to 544 nm in toluene phase is noticed as shown in Figure 1a, and it is attributed to the change of the polarity of the environment (solvent). The control experiment showed no dye transfer to toluene phase in the absence of **P3** or **P4**.

We estimated the maximum number of dye loading (N_{max}) per dendritic cores of **P3** and **P4** in toluene phase. Different molar ratios of AR-1 and **P3** or **P4** (polymer concentration, C_p, is from 0.1 to 15 μM) in water/toluene phases were shaken for 30 min and kept standing for 7 days at room temperature (to reach the constant absorbance value); the toluene phase was separated from the binary mixture and studied by UV−vis spectroscopic measurements. The concentrations of AR-1 solubilized in toluene phase were calculated from the maximum absorbance (λ_{max}) value at 544 nm by assuming the molar extinction coefficient (18 057 L mol^{-1} cm^{-1}) obtained for AR-1 in aqueous solution. From the AR-1 concentration in toluene, $[AR\text{-}1]_T$ and the corresponding known **P3** or **P4** concentrations, $[\mathbf{P}]_T$, one can calculate the number of dye molecules per dendritic micelle, $N_{max} = [AR\text{-}1]_T/[\mathbf{P}]_T$. Figure 1b shows the plots of N_{max} with initial molar ratio of AR-1 in water phase, $[AR\text{-}1]_w$, to $[\mathbf{P}]_T$, $N_{init} = [AR\text{-}1]_w/[\mathbf{P}]_T$. The maximum number of dye loading per dendritic core first increased with increasing N_{init}, reached a maximum, and tapered off to constant values at approximately 8 and 24 AR-1 molecules per dendritic core of **P3** and **P4**, respectively. From the above experiment it is evident that **P4** is a superior transporter to **P3**. It is also worth noting that at low dye to micelle ratio (1:1), **P4** effectively extracts all of the dye molecules from the aqueous layer, but **P3** extracts only approximately 40% (∼0.4 dye per micelle). The change of generation (size) of the dendritic cores is likely a crucial cause for this 3-fold increase in the dye transfer efficiency of **P4** against **P3**. This result is consistent with SAXS experimental facts that the volume of **P4** in toluene is 3-fold higher than that of **P3**. Another reason is likely due to that the higher hydrophobic coverage on the periphery of **P3** (∼72% against ∼51% on **P4**, as shown in the Experimental Section) might shield the entry of the polar dyes more effectively than for **P4**.

Although the transfer mechanism of dyes from aqueous phase to hydrophilic dendritic cores in nonpolar organic medium is not yet well-known, the most conceivable explanation as adopted by Cooper et al.[25] is that the hydrophilic core of highly plasticized dendritic micelle comes to the close proximity in the interface between two immiscible liquids, the water molecules diffuse into the dendritic cores, and the former accompanies the phase transfer of polar dye molecules. To estimate the role of water molecules two experiments were carried out. First is that AR-1 in dry powder form was directly added into toluene solution containing **P3,** and the solution was thoroughly shaken for 1 day at room temperature. One observed little entry of dye molecules into the supernatant toluene solution. The second experiment was to determine the number of water molecules inside **P4** by the Karl Fischer titration method. The toluene solution of **P4** (15−57 μM) was shaken for 30 min and kept for 7 days against excess amounts of water at room temperature. A blank experiment was also done for toluene in the absence of **P4**. After subtracting the quantity of water in the blank toluene solution (3.48 mM), one determines that a **P4** molecule in toluene contains 482−581 H_2O molecules.

Transport of Copper(II) Salt into Organic Phase via Complex Formation. The complexing ability of dendrimers to many different transition metal ions leads to the development of a new class of metallodendrimers.[21,37] Poly(amidoamine) (PAMAM) has a generation-dependent number of interior tertiary amines and is able to complex a range of metal ions including Cu(II), Pd(II), Pt(II), Ru(III), and Ni(II).[38−40] Here we report the sequestering ability of the PAMAM amphiphilic dendrimer to Cu(II) ions and effective removal of the latter from aqueous solution. 70.0 mg (3.2 μmol) of powdered **P3** was directly soaked into 10 mL of 10 mM Cu(II) salt solution for 7 days with constant stirring. After removal of the deep blue complex precipitated from the aqueous solution, the concentration of Cu^{2+} in the residual water phase was measured by UV−vis spectroscopy (using the λ_{max} at 810 nm and $\epsilon = 12.07$ L mol^{-1} cm^{-1}). A decrease in Cu(II) salt concentration

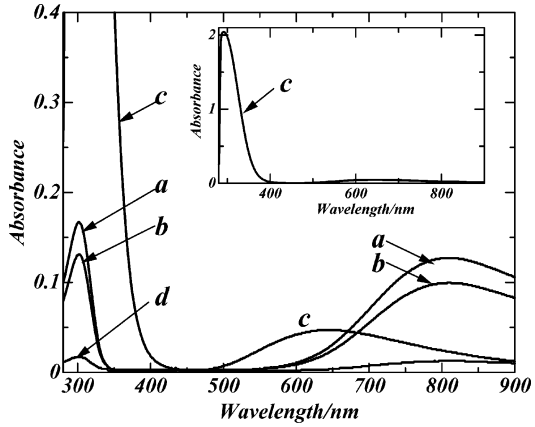

Figure 2. Absorption spectra of 10 mM aqueous Cu^{2+} solution before (spectrum a) and after (spectrum b) soaking with 70.0 mg of **P3** for 7 days [water as reference]. Spectrum c is the absorption spectra of the Cu(II) ions in toluene phase, transferred from the aqueous phase via the formation of complex with the dendrimer core in the presence ($[Cu(II)]_w/[\mathbf{P3}]_T = 200$ in aqueous/toluene phase), and spectrum d is that in the absence (blank) of amphiphilic dendrimer **P3** [toluene as reference].

(1.7 mM) in aqueous phase was noticed as shown in Figure 2 (curves a, b), and the capacity of encapsulation of Cu(II) salt by amphiphilic dendrimer solid was calculated to be 5.3 Cu(II) molecules per **P3**. The color of the complex remained unchanged after washing with water several times. We also examined the transfer of Cu(II) ions from aqueous phase to toluene phase containing **P3** via complex formation. Cu(II) salt and **P3** were mixed with a molar ratio of $[Cu(II)]_w = [8.0\ mM]$ to $[\mathbf{P3}] = [40\ \mu M]$ (mixed in equal (10 mL) volume of water to toluene phase) in aqueous/toluene medium and kept for 7 days at room temperature, after initial 30 min stirring. The transparent deep blue organic layer was separated from the mixture and studied by UV−vis spectroscopy. A new absorption peak was clearly observed at 646 nm (spectrum c in Figure 2), implying the effective transfer of Cu^{2+} ions from aqueous phase to organic phase. The blue shift of λ_{max} from 810 nm (d−d transition of Cu^{2+} ions in H_2O ligand field) to 646 nm and the appearance of a highly intense peak centered at 290 nm (ligand-to-metal charge transfer) prove the formation of complex of Cu^{2+} ions with PAMAM dendritic core.[41]

General Features of SAXS Profiles of P3 and P4 before and after Encapsulation of Polar Guest Molecules. SAXS is a well-accepted characterization tool, which allows one to study the internal structure as well as the interactions of polymer particles in solution phase. A relatively small number of reports on the intramolecular and/or intermolecular organization of dendritic structure by SAXS have been found in the literature.[42,43]

Scattering curves obtained from polymer solutions, after corrections for instrumental and solvent scattering effects, consist of scattering contributions from molecular size, shape, and intermolecular correlations.[44,45] The scattering from a group of monodisperse, globular particles in diluted solution can be expressed generally in terms of

$$\Delta I(q) = k^2 N P(q) \tag{1}$$

$$P(q) = \Delta I(q)/k^2 N \tag{2}$$

Table 1. Size of P3 in Toluene and Its Patent Dendrimer G3 in Methanol As Determined by SAXS at 25 °C[a]

P3 in toluene		**G3** in methanol	
C_p/mg/mL	R_g/Å	C_p/mg/mL	R_g/Å
0.818	17.4	0.920	16.1
4.28	17.8	1.65	16.2
8.70	17.7	2.97	16.1
		4.84	15.9
$(R_g)_{C_p=0} = 17.7$ Å		$(R_g)_{C_p=0} = 16.2$ Å	
$A_2 = 2.9_2 \times 10^{-4}$ mL mol/g^2		$A_2 = 6.4_0 \times 10^{-3}$ mL mol/g^2	
$A_{2,calcd} = 2.53 \times 10^{-4}$ mL mol/g^2		$A_{2,calcd} = 1.92 \times 10^{-3}$ mL mol/g^2	

[a] $A_{2,calcd}$ was calculated for a rigid sphere of radius R with the equation $A_{2,calcd} = 16 N_A \pi R^3/(3M^2)$, $R = (5/3)^{1/2} R_g$.

with the scattering vector, q, defined by

$$q = \frac{4\pi \sin\theta}{\lambda} \tag{3}$$

where θ is the scattering angle, λ the wavelength, $\Delta I(q)$ the experimental excess scattering intensity, k an electron density contrast factor, N the number of particles, and $P(q)$ the single particle scattering function.

Figure 3a,b displays representative SAXS profiles for amphiphilic dendrimers **P3** and **P4** in toluene without and with H_2O, AR-1, and Cu(II) salt solubilized inside the cores and also the corresponding parent dendrimers **G3** and **G4** in methanol at 25 °C. The SAXS profile of **P3** and **P4** in toluene is very similar to that of corresponding parent **G3** and **G4** in methanol, implying little structural difference between them. The scattering profile, however, significantly varies upon solubilizing polar guest molecules into **P3** and **P4** cores in toluene. The SAXS curves for the dendrimers after addition of polar guest molecules experience a shift of the first minimum to lower scattering vector magnitude, q, indicating the increase in the size of dendritic structures. This may be likely due to the swelling of the dendrimers in toluene upon solubilization of the water and polar molecules. In what follows, we first characterize some of the fundamental aspects of the hydrophobically modified dendrimers, **P3** and **P4,** in a selective solvent toluene, together with their parent dendrimers, **G3** and **G4,** in methanol as a good solvent by SAXS experiments. Subsequently, the conformational change upon the solubilization of polar guest molecules will be discussed.

Structural Characterization of Inverse Micelles of P3 and P4 in Toluene by SAXS. In the range where $qR_g < 1$, the intensity decay may be represented by Guinier's approximation and relate the radius of gyration R_g of the amphiphilic dendrimers via the following equation:

$$\Delta I(q) = \Delta I(0) \exp\left(-\frac{1}{3} R_g^2 q^2\right) \tag{4}$$

Figure 4a,b shows Guinier plots of the amphiphilic dendrimers **P3** and **P4** in toluene along with the corresponding parents **G3** and **G4** in methanol at 25 °C. It may be worth noting that straight line region in the plots appears to be held up to $qR_g \approx 2.5$ for **P3** and **G3** and ≈ 3.0 for **P4** and **G4,** respectively, to suggest particle anisotropy. From the initial slope of these plots, one can determine the values of R_g for all the macromolecules under study, and the data are listed in Tables 1 and 2. Figure 5a shows the plots of the R_g values against C_p for all corresponding dendritic macromol-

Table 2. Size of P4 in Toluene and Its Patent Dendrimer G4 in Methanol As Determined by SAXS at 25 °C[a]

P4 in toluene		**G4** in methanol	
C_p/mg/mL	R_g/Å	C_p/mg/mL	R_g/Å
1.77	25.6	1.07	20.3
3.91	25.6	1.62	20.4
6.70	25.1	2.46	20.0
9.12	24.8	4.05	19.8
$(R_g)_{C_p=0} = 25.9$ Å		$(R_g)_{C_p=0} = 20.6$ Å	
$A_2 = 7.0_4 \times 10^{-4}$ mL mol/g^2		$A_2 = 1.9_8 \times 10^{-3}$ mL mol/g^2	
$A_{2,calcd} = 2.98 \times 10^{-4}$ mL mol/g^2		$A_{2,calcd} = 9.41 \times 10^{-4}$ mL mol/g^2	

[a] $A_{2,calcd}$ was calculated for a rigid sphere of radius R with the equation $A_{2,calcd} = 16N_A\pi R^3/(3M^2)$, $R = (5/3)^{1/2}R_g$.

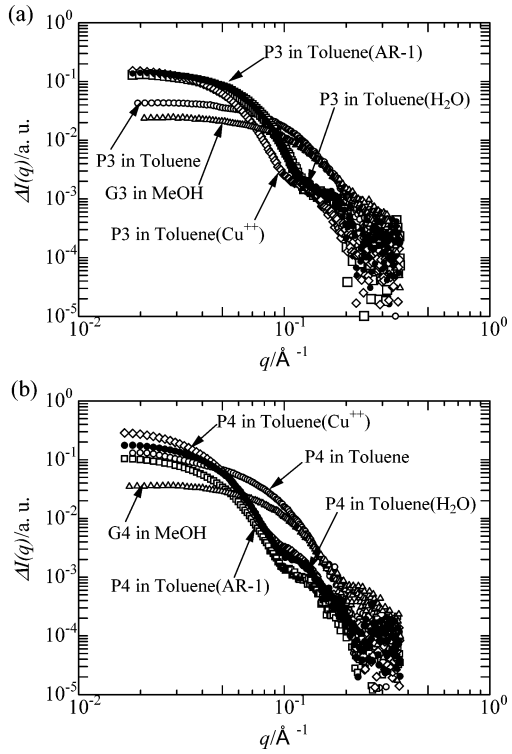

Figure 3. Small-angle X-ray scattering curves at 25 °C: (a) **G3** in MeOH (△), $C_p = 4.84$ mg/mL; **P3** in toluene (○), $C_p = 8.70$ mg/mL; **P3** in toluene (H_2O) (●), $C_p = 8.55$ mg/mL; **P3** in toluene (AR-1) (□), $C_p = 8.55$ mg/mL; **P3** in toluene (Cu(II)) (◊), $C_p = 8.55$ mg/mL: (b) **G4** in MeOH (△), $C_p = 4.05$ mg/mL; **P4** in toluene (○), $C_p = 9.12$ mg/mL; **P4** in toluene (H_2O) (●), $C_p = 8.60$ mg/mL; **P4** in toluene (AR-1) (□), $C_p = 8.60$ mg/mL; **P4** in toluene (Cu(II)) (◊), $C_p = 8.60$ mg/mL.

ecules. In this figure, a slight decrease of R_g values with increasing C_p is being noticed, and this is due to positive second virial coefficient in these solutions. To eliminate the concentration effects, the R_{g0} value at infinite dilution is determined via extrapolation to zero concentration. The values determined are also listed in Tables 1 and 2. It should be noted that the R_{g0} value of **P3** in toluene increases by 1.5 Å when compared to that of **G3** in methanol and that of **P4** increases by 5.3 Å against **G4**. The very slight increase in R_{g0} by addition of long octadecyl chains on the periphery of parent dendrimers might be explained by considering that either the alkyl chains are buried inside the dendritic cores or the dendritic core shrinks or collapses in toluene to show smaller R_g values than those for the original dendrimers in methanol as a good solvent.

Figure 5b shows the plots of $(C_p/\Delta I(q))_{q=0}$ vs C_p. From the intercept and slope one can determine second virial coefficient A_2. In this calculation one has to have a

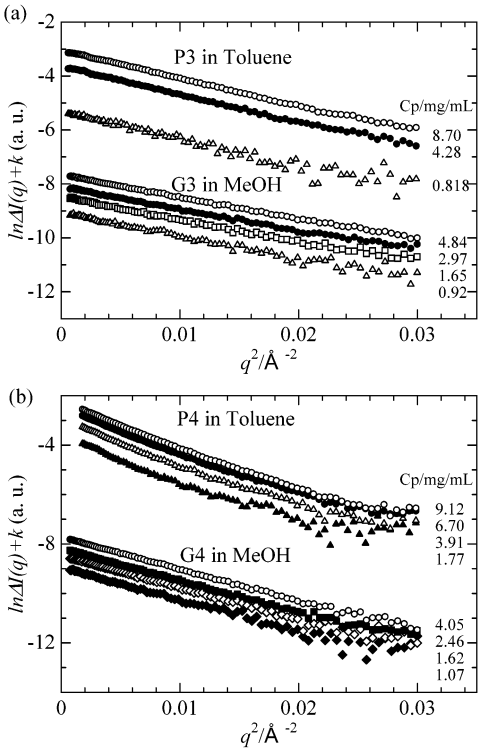

Figure 4. Guinier plots of the dendrimer solutions with different concentrations at 25 °C: (a) **G3** in MeOH and **P3** in toluene; (b) **G4** in MeOH and **P4** in toluene.

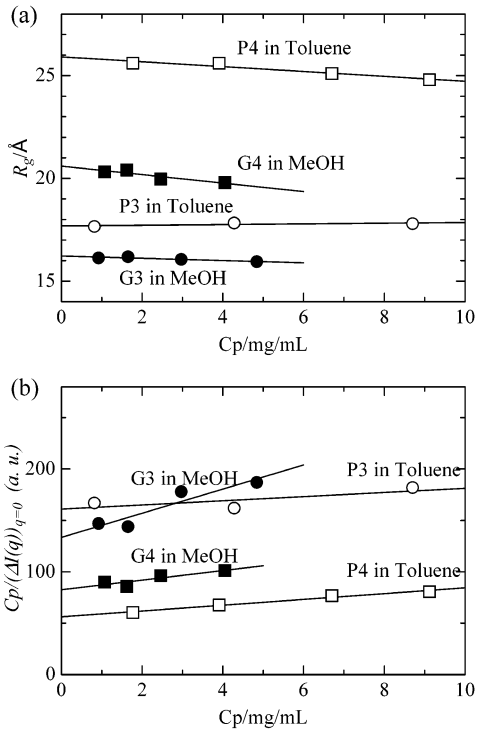

Figure 5. (a) Plots of R_g against C_p for the various dendrimers: (●) **G3**, (○) **P3**, (■) **G4**, and (□) **P4**. **(b)** Plots of $(C_p/\Delta I(q))_{q=0}$ vs C_p: (●) **G3**, (○) **P3**, (■) **G4**, and (□) **P4**.

assumption for the molecular weight of **P3** and **P4**, although we did not experimentally determine it. One used the calculated molecular weights (shown in the Experimental Section). The experimental data of A_2 and theoretical values calculated for rigid sphere are summarized in Tables 1 and 2. The positive A_2 values of both **P** in toluene and corresponding **G** in methanol are

Table 3. Characteristics of P3 and P4 with Encapsulated Polar Guest Molecules Inside the Dendritic Cores at 25 °C

P3 in toluene				**P4** in toluene			
C_p/mg/mL	guest molecule	R_g/Å	$\Delta I(0)$/au	C_p/mg/mL	guest molecules	R_g/Å	$\Delta I(0)$/au
0.00		17.7		0.00		25.9	
8.55	AR-1	27.6	0.14_9	8.60	AR-1	37.6	0.12_2
8.55	Cu	34.5	0.17_7	8.60	Cu	43.2	0.34_7
8.55	H_2O	28.0	0.15_9	8.60	H_2O	37.0	0.20_8

experimentally obtained, and these are larger than ones calculated for a hard sphere.

The scattering form factor $P(q) = \Delta I(q)/\Delta I(0)$ of SAXS data for the dendrimer molecules may be compared with a monodisperse system of sphere and ellipsoids of revolution. For sphere with radius R

$$P(q)_{\text{sphere}} = \Phi^2(q) = \left[\frac{3(\sin x - x\cos x)}{x^3}\right]^2 \quad (5)$$

$$R_g{}^2 = \frac{3}{5}R^2 \quad (6)$$

where $x = qR$. Similarly, for monodisperse ellipsoids of revolution with a and νa

$$P(q)_{\text{ellipsoid}} = \int_0^{\pi/2} \Phi^2(qa\sqrt{\cos^2\theta + \nu^2\sin^2\theta})\cos\theta\, d\theta \quad (7)$$

$$R_g{}^2 = \frac{2+\nu^2}{5}a^2 \quad (8)$$

Comparison in Kratky plots between experimental data and the theoretical curves calculated from eqs 5−8 of third generation dendrimers as well as their amphiphilic derivatives are shown in Figure 6a,b. When compared directly to the experimental scattering curve in these figures, the sphere and ellipsoids of revolution model with constant density are not able to fit the data very well. It may be fair to say, however, that the simple ellipsoids of revolution models at least qualitatively describe SAXS experimental scattering profiles for low generation dendrimers. When the soft-sphere model like star model[46] is also applied to the present experimental profiles, similar disagreement between the model scattering prediction and experimental results is obtained.[43] Since the polydispersity of the present dendrimer samples significantly influences the scattering profile, the effect should be carefully taken into account assuming an appropriate distribution function with other parameters.[43] It may be concluded from the comparison in the experimental profiles between **G3** and **P3** that **P3** assumes more globular spherical conformation in selective solvent than **G3** in good solvent. Similar results are also obtained for fourth generation dendrimers, **G4** and **P4**.

Structural Characterization of P3 and P4 Having Polar Guest Molecules Inside. The SAXS profiles for the dendrimers after loading polar guest molecules such as water, AR-1, and Cu(II) salt significantly differ from that before loading, as shown in Figure 3. It is clearly seen that the encapsulation of polar molecules increases the size of dendrimer molecules. Table 3 shows the values of R_g for **P3** and **P4** in toluene after solubilization of H_2O, AR-1, and Cu(II) salt. In fact, the R_g values of the amphiphilic dendrimer molecules in toluene are remarkably increased by encapsulation of the polar molecules. Water molecules, good solvent for the core but not solvent for long alkyl chain, increase

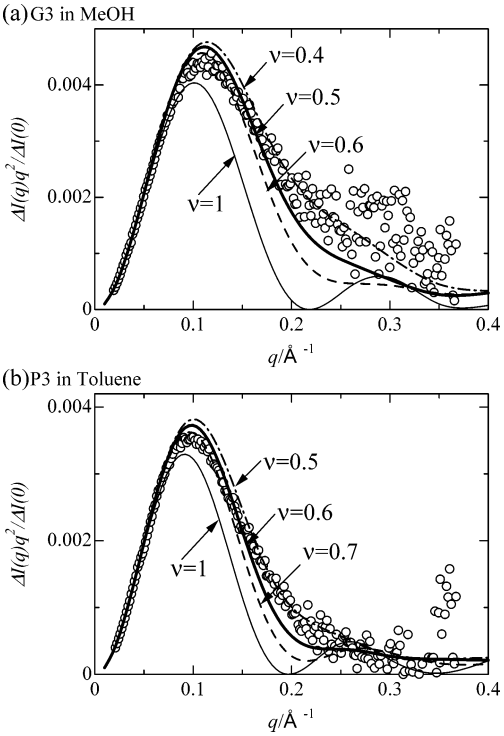

Figure 6. Comparison of experimental SAXS data with theoretical curves calculated from eqs 5−8. (a) **G3** in MeOH, $C_p = 4.84$ mg/mL, thin solid line: sphere ($\nu = 1$), chain lines: $\nu = 0.4$, thick solid line: $\nu = 0.5$, and broken lines: $\nu = 0.6$. (b) **P3** in toluene, $C_p = 8.70$ mg/mL: thin solid line, sphere ($\nu = 1$); chain lines, $\nu = 0.5$; thick solid line, $\nu = 0.6$; broken lines, $\nu = 0.7$.

the volume of **P3** by 4-fold and **P4** by 3-fold. They may diffuse into the originally globular core in toluene to solvate the dendritic segments and swell it. They may also concurrently push the buried long alkyl chains out the toluene phase to transform the definite core−shell sphere consisting of a dendritic core swollen by water and alkyl chains swollen by continuous solvent. Since the numbers of AR-1 molecules inside the core are mostly 8−24, AR-1 molecules are thought to be not so effective in the core chain expansion. Interestingly, further chain expansion by the presence of Cu(II) ions is observed and most likely due to complex formation with amine groups in the dendritic core or increase of water content. The discussion of the partial oligomerization with N−Cu−N bridges occurred may be roughly carried out by comparing the values of $\Delta I(0)$ at the constant C_p as listed in Table 3. It can be inferred that **P3** molecules do not take place any intermolecular oligomerization upon the complexation with Cu(II) in toluene within experimental error. In the case of **P4**, a slight increase in $\Delta I(0)$ with Cu(II) and decrease in $\Delta I(0)$ with AR-1 are most likely due to the difference in the electron density contrast factor, k, in eq 1 between H_2O only and H_2O + polar materials. Eventually, the partial oligomerization of the present low generation dendrimers by complexing with Cu ions seems unlikely. Light

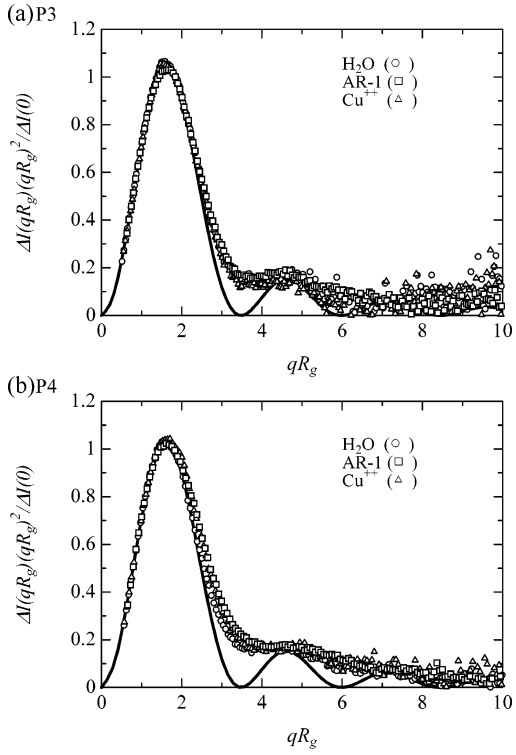

Figure 7. Comparison of experimental SAXS data of amphiphilic dendrimers in toluene in the presence of polar guest molecules with theoretical curves calculated with sphere model: (a) **P3**, $C_p = 8.55$ mg/mL, H_2O (○), AR-1 (□), and Cu(II) (△); (b) **P4**, $C_p = 8.60$ mg/mL, H_2O (○),AR-1 (□), Cu(II) (△).

scattering experiments about this subject are now under study.

Figure 7 shows comparison in the Kratky plots of the experimental data of **P3** and **P4** with the theoretical curve calculated for the sphere model with constant density by using eq 5. The figures clearly demonstrate that the experimental scattering profile of **P3** and **P4** molecules after solubilization of polar molecules can be semiquantitatively described in terms of the sphere model. The core−shell model[47] with four new parameters, electron density of core and shell, and their sizes may also describe the present experimental data. The slight deviations from a theoretical curve in the region of $3 < qR_g < 4.3$ are likely due to the polydispersity of the sample or/and simple sphere model with constant density.

A conclusive picture that comes from all experiments mentioned in this study is presented in Figure 8. **P3** and **P4** molecules in toluene assume a conformation similar to **G3** and **G4** in methanol, irrespective of the presence of long alkyl chains in the formers. The SAXS scattering profiles of these particles are likely described by the ellipsoids of revolution. Water molecules solubilized into the core of **P3** and **P4** remarkably expand their chain conformation in toluene. The chain conformation was further expanded by the presence of Cu^{2+}, probably due to complex formation. The number of water molecules inside a **P4** is 482−581, which corresponds to water droplet with 15−16 Å in radius and 10−12% of the increase in volume. Water molecules encapsulated push the long stearyl chains originally buried inside the dendritic cores out toluene phase to afford a definite core−shell sphere. The scattering profiles of expanded **P3** and **P4** are semiquantitatively described in terms of sphere model with constant density. The dendritic box can effectively transfer AR-1 molecules from water to toluene phase and the maximum number per dendrimer is 8 for **P3** and 24 for **P4**. The increase in dye loading from **P3** to **P4** is consistent with the relation of the particle volume before and after loading.

Conclusions

Hydrophilic PAMAM dendrimers of **G3** and **G4** were successfully converted to amphiphilic units **P3** and **P4**, respectively, by hydrophobic surface modification with stearyl acrylates. Amphiphilic dendrimers form unimolecular inverse micelle structure in toluene solution and effectively hosted the transfer of polar organic dye AR-1 as well as Cu(II) salt from aqueous phase to toluene phase. The maximum number of dye loading per dendritic core was estimated and almost 3-fold increase in efficacy of **P4** having higher generation (size) cores over **P3** was found. The SAXS data revealed the unimolecular nature of the inverse micelles formed by **P3** and **P4**

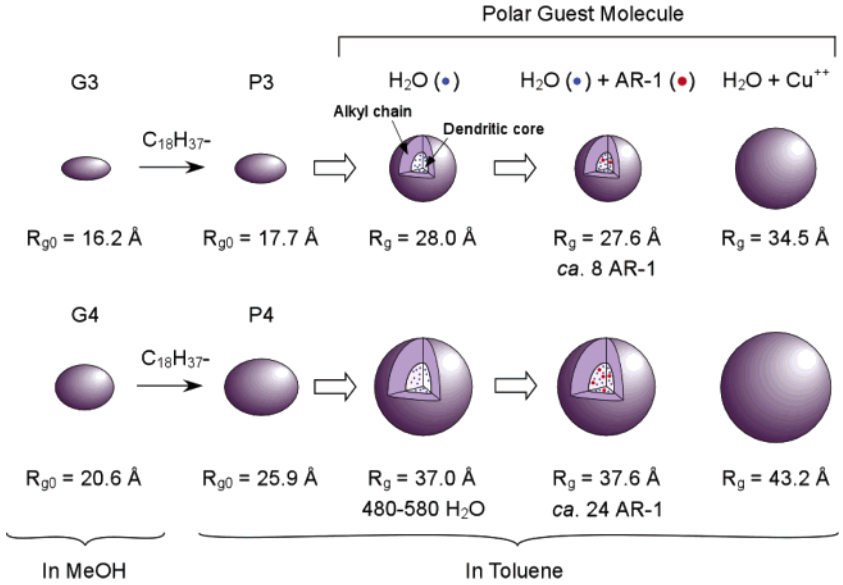

Figure 8. Schematic representations of developments of amphiphilic dendrimer molecules by encapsulation of polar guest molecules in toluene.

in toluene, with a collapsed core of ellipsoids of revolution having an average radius of gyration 17.7 and 25.9 Å, respectively. The solubilization of water and AR-1 molecules expands the core to assume to be almost matching with sphere model. Pronounced effects of encapsulated Cu(II) ions on the chain expansion were observed and attributed to the complex formation of dendritic cores with Cu(II) ions.

Acknowledgment. This work was supported in part by a Grant-in-Aid (No.13650943) from the Ministry of Education, Science, Culture and Sports, Japan, Saneyoshi Scholarship Foundation, and Eno Science Foundation.

References and Notes

(1) Tomalia, D. A.; Baker, H.; Dewald, J.; Hall, M.; Kallos, G.; Martin, S.; Roeck, J. *Polym. J.* **1985**, *17*, 117.
(2) de Brabander-van den Berg, E. M. M.; Meijer, E. W. *Angew. Chem., Int. Ed. Engl.* **1993**, *32*, 1308.
(3) Fischer, M.; Vögtle, F. *Angew. Chem., Int. Ed.* **1999**, *38*, 884.
(4) Schluter, A. D.; Rabe, J. P. *Angew. Chem., Int. Ed.* **2000**, *39*, 864.
(5) Tomalia, D. A.; Kaplan, D. A.; Kruper, W. J., Jr.; Cheng, R. C.; Tomlinson, I. A.; Fazio, M. J.; Edwards, D. S. US Patent 5 728 461, 1994.
(6) Knapen, J. W. J.; can der Made, A. W.; de Wilde, J. C.; van Leeuwen, P. W. N. M.; Wijkens, P.; Grove, D. M.; van Koten, G. *Nature (London)* **1997**, *372*, 659.
(7) Bielinska, A.; Kukowska-Latallo, J. F.; Johnson, J.; Tomalia, D. A.; Baker, J. R., Jr. *Nucleic Acids Res.* **1996**, *24*, 2176.
(8) Bar-Haim, A.; Klafter, J.; Kopelman, R. *J. Am. Chem. Soc.* **1997**, *119*, 6197.
(9) Wells, M.; Crooks, R. M. *J. Am. Chem. Soc.* **1996**, *118*, 3988.
(10) Mathews, O. A.; Shipway, A. N.; Stoddart, J. F. *Prog. Polym. Sci.* **1998**, *23*, 1.
(11) Newkome, G. R.; Moorefield, C. N.; Baker, G. R.; Saunders, M. J.; Grossman, S. H. *Angew. Chem., Int. Ed. Engl.* **1991**, *30*, 1178.
(12) Moreno-Bondi, M. C.; Orellana, G.; Turro, N. J.; Tomalia, D. A. *Macromolecules* **1990**, *23*, 910.
(13) Ottaviani, M. F.; Cossu, E.; Turro, N. J.; Tomalia, D. A. *J. Am. Chem. Soc.* **1995**, *117*, 4387.
(14) Newkome, G. R.; Yao, Z.-Q.; Baker, G. R.; Gupta, V. K. *J. Org. Chem.* **1985**, *50*, 2003.
(15) Hawker, C. J.; Wooley, K. L.; Fréchet, J. M. J. *J. Chem. Soc., Perkin Trans. I* **1993**, 1287.
(16) Matteis, S.; Seiler, P.; Diederich, F.; Gramlich, V. *Helv. Chim. Acta* **1995**, *78*, 1904.
(17) Stevelmans, S.; van Hest, J. C. M.; Jansen, J. F. G. A.; van Boxtel, D. A. F. J.; de Branbander-van den Berg, E. M. M.; Meijer, E. W. *J. Am. Chem. Soc.* **1996**, *118*, 7398.
(18) Lochmann, L.; Wooley, K. L.; Ivanova, P. T.; Fréchet, J. M. J. *J. Am. Chem. Soc.* **1993**, *115*, 7043.
(19) Liu, M.; Fréchet, J. M. J. *Polym. Bull. (Berlin)* **1999**, *43*, 379.
(20) Sayed-Sweet, Y.; Hedstrand, D. M.; Spinder, R.; Tomalia, D. A. *J. Mater. Chem.* **1997**, *7*, 1199.
(21) Gröhn, F.; Bauer, B. J.; Amis, E. J. *Macromolecules* **2001**, *34*, 6701.
(22) Bosman, A. W.; Janssen, H. M.; Meijer, E. W. *Chem. Rev.* **1999**, *99*, 1665.
(23) Baars, M. W. P. L.; Froehling, P. E.; Mijer, E. W. *Chem. Commun.* **1997**, 1959.
(24) Krska, S. W.; Seyferth, D. *J. Am. Chem. Soc.* **1998**, *120*, 3604.
(25) Cooper, A. I.; Londono, J. D.; Wignall, G.; McClain, J. B.; Samulski, E. T.; Lin, J. S.; Dobrynin, A.; Rubinstein, M.; Burke, A. L. C.; Frechet, J. M. J.; DeSimone, J. M. *Nature (London)* **1997**, *389*, 368.
(26) Naylor, A. M.; Goddard, W. A.; Kiefer, G. E.; Tomalia, D. A. *J. Am. Chem. Soc.* **1989**, *111*, 2339.
(27) Sui, G.; Micic, M.; Huo, Q.; Leblanc, R. M. *Colloids Surf. A: Physicochem. Eng. Aspects* **2000**, *171*, 185.
(28) Sui, G.; Micic, M.; Huo, Q.; Leblanc, R. M. *Langmuir* **2000**, *16*, 7847.
(29) Crooks, R. M.; Lemon III, B. I.; Sun, L.; Yeung, L. K.; Zhao, M. *Top. Curr. Chem.* **2001**, *212*, 81.
(30) Schenning, A. P. H. J.; Elissen-Roman, C.; Weener, J. W.; Baars, M. W. P. L.; vander Gast, S. J.; Meijer, E. W. *J. Am. Chem. Soc.* **1998**, *120*, 8199.
(31) Ruckenstein, E.; Yin, W. *J. Polym. Sci., Polym. Chem. Ed.* **2000**, *38*, 1443.
(32) Ueki, T,; Hiragi, Y.; Kataoka, M.; Inoko, Y.; Amemiya, Y.; Izumi, Y.; Tagawa, H.; Muroga, Y. *Biophys. Chem.* **1985**, *23*, 115.
(33) Baars, M. W. P. L.; Meijer, E. W. *Top. Curr. Chem.* **2000**, *210*, 131.
(34) Jansen, J. F. G. A.; de Brabander-van den Berg, E. M. M.; Meijer, E. W. *Science* **1994**, *266*, 1226.
(35) Jansen, J. F. G. A.; Meijer, E. W. *J. Am. Chem. Soc.* **1995**, *117*, 4417.
(36) Boas, U.; Karlsson, A. J.; de Waal, B. F. M.; Meijer, E. W. *J. Org. Chem.* **2001**, *66*, 2136.
(37) Newkome, G. R.; He, E. F.; Moorefield, C. N. *Chem. Rev.* **1999**, *99*, 1689.
(38) Ottaviani, M. F.; Montalti, F.; Turro, N. J.; Tomalia, D. A. *J. Phys. Chem. B* **1997**, *101*, 158.
(39) Zhao, M.; Sun, L.; Crooks, R. M. *J. Am. Chem. Soc.* **1998**, *120*, 4877.
(40) Balogh, L.; Tomalia, D. A. *J. Am. Chem. Soc.* **1998**, *120*, 7355.
(41) Cotton, F. A.; Wilkinson, G. *Advances in Inorganic Chemistry*; Wiley: New York, 1980; pp 815−817.
(42) Prosa, T. J.; Bauer, B. J.; Amis, E. J.; Tomalia, D. A.; Scherrenberg, R. J. *J. Polym. Sci., Part B: Polym. Phys.* **1997**, *35*, 2913.
(43) Prosa, T. J.; Bauer, B. J.; Amis, E. J. *Macromolecules* **2001**, *34*, 4897.
(44) Guinier, A.; Fournet, G. *Small Angel Scattering of X-Rays;* Wiley: New York, 1955.
(45) Glatter, O.; Kratky, O. *Small Angel X-Ray Scattering;* Academic Press: New York, 1982.
(46) Burchard, W. *Macromolecules* **1977**, *10*, 919.
(47) Friman, R.; Rosenholm, J. B. *Colloid Polym. Sci.* **1982**, *260*, 545.

MA0343075